DOI 10.1007/s11204-017-9436-6
Soil Mechanics and Foundation Engineering, Vol. 54, No. 2, May, 2017 (Russian Original No. 2, March-April, 2017)

SOIL MECHANICS

ANALYSIS OF STRIP PILE FOOTING BEHAVIOR CAUSED BY SINKHOLE FORMATION

UDC 55.144:624.131.522.34

N. Z. Gotman[1] and D. A. Davletyarov[2]
[1]Perm State University, Perm. Russia; [2]LLC "Podzemproekt", Moscow, Russia.

The paper presents the results of investigation of pile strip footing behavior over a karst sinkhole. Analytical decisions based on the adapted contact model of pile-subsoil interaction were obtained to evaluate the pile stiffness coefficient and maximal loads acting on the piles.

Introduction

Safety of buildings and structures in karst-prone areas is mostly ensured by so-called "karst-safe" strip pile footings. To design such footings, numerical simulations of non-uniform settlements of subsoil are required. Because of inherently limited and approximate data on soil deformation and strength parameters, only primitive mathematical models are used for such calculations, i.e., the specific contact model, which simulates piles as a kind of "finite stiffness links," similarly to the stiffness coefficient of the pile.

Research [1] shows that the stiffness coefficient for piles located near the potential sinkhole should be different from that designed for normal conditions. Specific theoretical and experimental investigations of strip pile footing behavior near a karst sinkhole were performed to obtain an analytical decision for evaluation the pile stiffness coefficient in such cases.

Behavior of piles around a karst cavity

A series of numerical investigations of behavior of axially loaded piles around a karst cavity, simulated as a stepped funnel, was conducted (Fig. 1).

A soil massif reinforced with piles was simulated using "PLAXIS 3D Foundation" software with hardening elasto-plastic model of soil stress-strain behavior and 3D finite elements, combined with 2D pile-soil interface elements (Fig. 2).

The obtained data are shown as "load-settlement" curves for various combinations of pile length, depth of sinkhole, and pile-to-sinkhole distance. Based on the "load – settlement" diagrams, the coefficient of pile stiffness was determined as pile load over pile settlement ratio at the end point of the "quasi-linear" part of the graph. The shape variation of the "load – settlement" curve reflects the changing operational conditions for piles around the cavity. The quantitative parameter of this variation is determined as $\alpha = K/K_1$, where K and K_1 are the stiffness ratios prior to and after the karst sinkhole formation, respectively.

The main variable parameters in the numerical investigations are the pile length (l_p) over the karst cavity depth (H_k) ratio, pile to cavity edge distance (S), and subsoil parameters.

Translated from Osnovaniya, Fundamenty i Mekhanika Gruntov, No. 2, pp. 2-5, March-April, 2017.
0038-0741/17/5402-0071

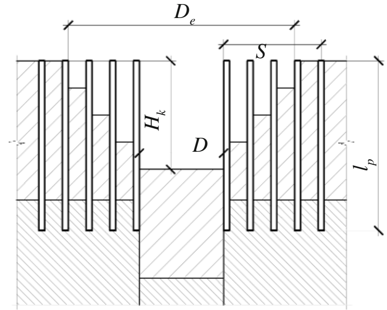

Fig. 1. Strip pile footing on subsoil with a karst sinkhole.

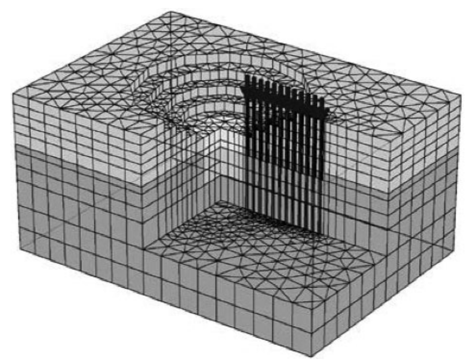

Fig. 2. 3D FEM model "PLAXIS 3D Foundation" software.

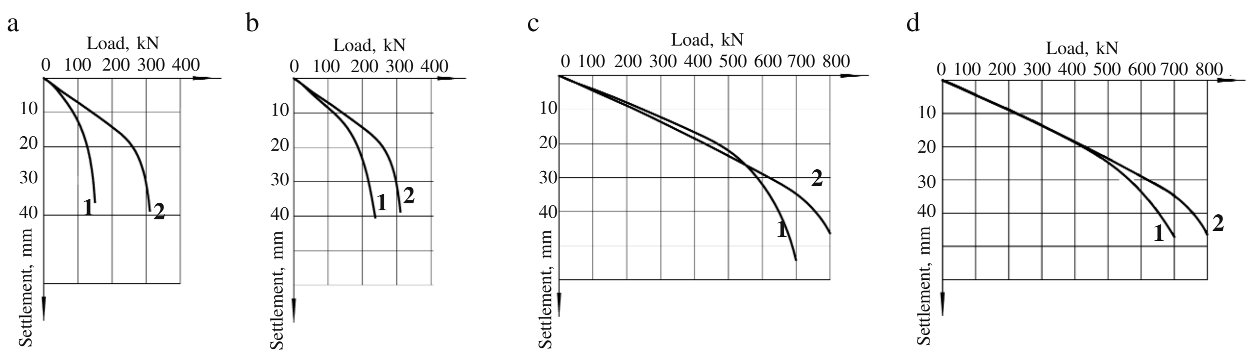

Fig. 3. Load-settlement relationships for the first type of subsoil: a) l_p/H_k = 0.553; S = 0.5 m; b) l_p/H_k = 0.553; S = 3.5 m; c) l_p/H_k = 1.515; S = 0.5 m; d) l_p/H_k = 1.515; S = 3.5 m; 1) with the account of carst cavity and 2) without the account of carst cavity.

The simulation involved 40 variants of initial data with l_p ranging from 6 to 16 m, S = 0.5-8 m, and H_k = 6-10 m. Two types of two-layer subsoil were investigated: 1) soft plastic clay loam (below the surface) and semihard clays (below the lower pile tip); 2) soft plastic clay loams (below the surface) and gravelly soil (below the lower pile tip).

Figure 3 shows the "load-settlement" curves for the first type of subsoil with l_p/H_k = 0.553 and 1.515 for pile-sinkhole edge distance S = 0.5 m and 3.5 m, respectively. Table 1 and Fig. 4a show the results of calculating α depending on l_p/H_k and S/H_k. The curves were approximated as

$$\alpha = 1 + \frac{m}{(l_p/H_k)^2}, \tag{1}$$

where m is determined from the S/H_k ratio (see Fig. 4b):

$$m = \frac{0.041}{(S/H_k)^2 + 0.04}. \tag{2}$$

TABLE 1

l_p/H_k	Coefficient α at S/H_k equal to							
	0.049	0.146	0.243	0.340	0.437	0.534	0.631	0.728
0.553	4.103	2.487	2.205	1.590	1.385	1.128	1.077	1
0.777	2.583	1.917	1.792	1.542	1.458	1.250	1.167	1
0.971	2.000	1.824	1.735	1.412	1.294	1.059	1.059	1
1.165	1.500	1.417	1.417	1.292	1.250	1.125	1.042	1
1.515	1.125	1.125	1.125	1.125	1.125	1.063	1.063	1

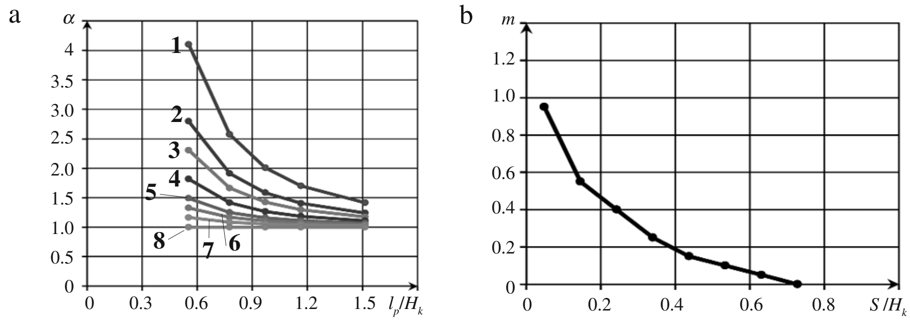

Fig. 4. Dependence of α on l_p/H_k (a) and m on S/H_k (b): S/H_k = 0.049 (1); 0.146 (2); 0.243 (3); 0.340 (4); 0.437 (5); 0.534 (6); 0.631 (7); 0.728 (8).

TABLE 2

Sands		Coefficient β at void ratio e equal to						
		0.45	0.55	0.65	0.75	0.85	0.95	1.05
Gravelly and coarse grained		0.25	0.39	0.54	–	–	–	–
Medium grain size		0.27	0.42	0.56	–	–	–	–
Fine		0.27	0.53	0.79	1.05	–	–	–
Silty		0.35	0.69	1.03	1.37	–	–	–
Sand loams	$0 \le I_L \le 0.25$	0.73	0.96	1.21	1.46	–	–	–
	$0.25 < I_L \le 0.75$	0.77	0.98	1.18	1.47	1.84	–	–
Clay loams	$0 \le I_L \le 0.25$	0.56	0.79	0.91	1.08	1.21	1.44	–
	$0.25 < I_L \le 0.5$	0.68	0.84	1.00	1.21	1.46	1.69	–
	$0.5 < I_L \le 0.75$	–	–	1.11	1.37	1.64	1.85	2.06
Clays	$0 \le I_L \le 0.25$	–	0.71	0.83	0.93	1.04	1.19	1.34
	$0.25 < I_L \le 0.5$	–	–	0.88	1.00	1.17	1.36	1.61
	$0.5 < I_L \le 0.75$	–	–	1.05	1.19	1.40	1.60	1.78

Inserting m from (2) into (1) followed by some mathematical transformations allows us to determine the factor α that reduces the pile stiffness factor until the moment of formation of the karst cavity:

$$\alpha = 1 + \frac{0.041 H_k^4}{l_p^2 (S^2 + 0.04 H_k^4)}. \tag{3}$$

To account for the soil conditions, the coefficient β was introduced in Eq. (3) using the results of the numerical analysis (Fig. 3):

$$\alpha = 1 + \beta \frac{0.041 H_k^4}{l_p^2 (S^2 + 0.04 H_k^4)}. \tag{4}$$

The calculations were followed by evaluation of β in sand and clay soils (Table 2) with different physical and mechanical properties.

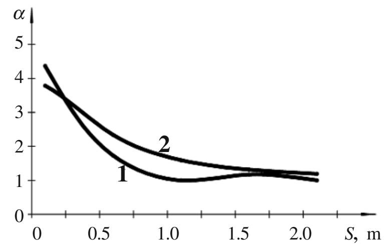

Fig. 5. Variation of α versus S: 1) in-situ test data; 2) the results of Eq. (4).

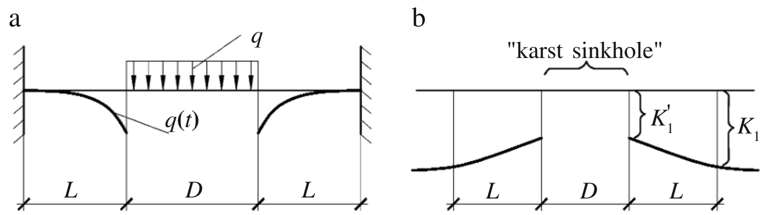

Fig. 6. Diagram of load distribution (a) and of pile stiffness ratio (b) over karst sinkhole.

The values of α calculated using Eq. (4) were compared with the results of in-situ tests of pile footing fragments.

Reinforced concrete 150×150×3000 mm piles were used in the investigations. The test site soils were represented by semisolid clay loams. Karst sinkholes were simulated by artificial excavation of the corresponding volume of soil. The footings were tested by two consecutive static load tests, one of which was continued until the cavity formation and the other, after. The load-settlement curves were plotted based on the in-situ experimental data, and the reduction of the pile stiffness factors ($\alpha = K/K_1$) was evaluated for the case of sinkhole formation, depending on the pile-sinkhole distance S.

Figure 5 demonstrates satisfactory consistency between analytical and test data.

As a result, it was proposed to reduce the stiffness ratio coefficient (K_1) of piles located near a sinkhole as compared to the stiffness ratio coefficient (K) determined for normal operating conditions, i.e., when a sinkhole under a footing does not form. The coefficient K_1 depends on l_p, H_k, S, as well as on soil parameters in the subsoil layers:

$$K_1 = K / \left(1 + \beta \frac{0.041 H_k^4}{l_p^2 (S^2 + 0.04 H_k^2)}\right). \tag{5}$$

Evaluation of maximum loads on piles in the case of karst sinkhole formation

When a karst sinkhole forms under a pile strip footing, the load from the upper structures is redistributed on the piles near the sinkhole, as is shown on Fig. 6a, while the stiffness ratio decreases (Fig. 6b). The extra load acting on the piles around the sinkhole (q_t) is redistributed on the piles at distance L. The value of L depends on the pile raft stiffness, the diameter of the karst sinkhole, and the pile stiffness ratio. It can be determined [2] on the basis of the following equation:

$$L^3 = \frac{36 B(t)}{D K(t)}, \tag{6}$$

where $B(t)$ is the raft stiffness; $K(t)$ is the stiffness ratio of piles near the sinkhole.

In the case of a strip pile footing with a raft of rectangular cross section and height h, we have

$$L = \sqrt[3]{\frac{3E_c abh^3}{K_1^1 D}}, \qquad (7)$$

where K_1^1 is the minimum stiffness ratio for the piles around the sinkhole (Fig. 6b); E_c is the deformation modulus of the concrete; b is the raft width; a is the pile spacing.

The extra load acting on the pile raft is distributed over a triangular diagram along the segment with length of L (Fig. 6a), decreasing from the maximum value at the edge of the karst sinkhole to zero at the borders of the segment. The stiffness ratio K_1^1 near the sinkhole edge can be determined from Eq. (5) when $S = 0$ and $H_k^2/l_p^2 = \gamma$

$$K_1^1 = K/(1 + \beta\gamma). \qquad (8)$$

The additional load

$$\Delta N = (3qD_a)/(2L). \qquad (9)$$

Considering Eqs. (7)-(9) jointly, we obtain an equation for evaluating the maximum extra load on the pile when the karst sinkhole forms:

$$\Delta N = \frac{3qD_a}{2h}\sqrt[3]{\frac{KD}{3E_c ab(1+\beta\gamma)}}. \qquad (10)$$

Thus, the maximum load on piles with account of the karst sinkhole formation is

$$P_{\max} = P + \Delta N, \qquad (11)$$

where P is the load acting on the pile calculated for normal operating conditions, i.e., without account of karst sinkhole formation.

The use of the proposed analytical equations enabled the maximum loads acting on the piles around the karst sinkhole to be evaluated without time-consuming calculations and allowed the spacing and length of piles to be preliminary determined. This is most valuable for design optimization.

The analytical solutions for K and $P_{\max}$ were applied for the design of pile footings of a trade center in Ufa city. Taking account of the reduction of pile stiffness ratio near the sinkhole enabled decreasing the evaluation of maximum load values acting on the piles around the sinkhole and reducing the number of piles by 30% as compared to conventional calculations.

Conclusions

1. As the result of the research, new analytical solutions were developed for calculating the stiffness ratio of piles around a karst sinkhole as a function of pile length, sinkhole depth, pile to sinkhole edge distance, as well as soil parameters of the cover stratum.

2. An analytical method for evaluating maximum loads on piles surrounding a karst sinkhole was proposed, which allows the spacing and lengths of the footing piles around the karst sinkhole to be predetermined with no time-consuming computations. This is most valuable for optimization of the design process.

REFERENCES

1. N. Z. Gotman, "Analysis of anti-karst footings of buildings and structures," *Osn. Fundam. Mekh. Gruntov*, No. 1, 20-24 (2008).
2. I. S. Metelyuk, "An engineering method for a karst sinkhole impact on footings of frameless buildings," *Stroit. Konstr.*, No. 42, 6-11 (1989).